

Scattering-Controlled Transmission Resonances and Negative Differential Conductance by Field-Induced Localization in Superlattices

Fabio Beltram, Federico Capasso, Deborah L. Sivco, Albert L. Hutchinson, Sung-Nee G. Chu, and Alfred Y. Cho

AT&T Bell Laboratories, Murray Hill, New Jersey 07974

(Received 27 February 1990)

The first observation of scattering-controlled transmission resonances in superlattices is reported. These originate from states supported by subsets of the superlattice of thickness equal to the electron coherence length. At lower electric fields a broad region of negative differential conductance due to progressive field-induced wave-function localization is also observed. This phenomenon is shown to be physically equivalent to the Bragg-diffraction-induced negative differential conductance predicted by Esaki and Tsu in 1970.

PACS numbers: 73.20.Dx, 73.40.Gk, 73.50.Fq

Since the original proposal of superlattices (SL's) by Esaki and Tsu,¹ transport in these structures has been the object of intense investigations. When an electric field F is applied to a SL of period a , some different transport regimes are commonly identified.² At low fields, the current increases linearly with field (mobility regime). The current is expected to decrease with increasing field when the electron distribution probes the negative-mass region of the miniband, i.e., according to Esaki and Tsu,¹ for

$$F > \hbar/ea\tau, \quad (1)$$

where τ is the scattering time and e is the electron charge. This behavior is caused by the fact that an increasing fraction of the carriers approaches the minizone boundary therefore undergoing Bragg diffraction. Equation (1) was shown to hold independently of the details of the miniband energy dispersion relation.³

Another regime was studied by Tsu and Döhler,⁴ who considered the case of strong localization in a tight-binding SL (i.e., a SL with weak coupling between wells). They showed that due to the decreasing overlap between the wave functions of adjacent wells, the transition rate due to hopping (and therefore the current) decreases with increasing field for

$$F > \Delta E/ea, \quad (2)$$

where ΔE is the miniband width.

In this Letter we present direct evidence of negative differential conductance (NDC) by electric-field-induced localization in SL's and show that this mechanism and the Bragg-diffraction-induced NDC predicted by Esaki and Tsu are physically equivalent. Furthermore, we report the first observation of new resonances that are determined by scattering.

One must not be led to the incorrect notion that Eq. (2) is a *necessary* requirement for the observation of localization in transport.⁵⁻⁷ Even for fields much lower than those causing the complete localization mentioned above, a progressive localization of the electronic states is to be expected. As originally discussed by Wannier,⁸ and subsequently by Kazarinov and Suris⁹ in the context

of transport in SL's, in an electric field the electronic wave functions extend over a number of periods of the order of $\Delta E/eaF$ and are separated in energy by eaF [the so-called Wannier-Stark ladder, Fig. 1(a)]. Thus, as the field is increased the wave functions become increasingly localized in space up to the extreme point where they are shrunk to one well. This is the limit of Eq. (2) in which the SL consists of a "ladder" of identical isolated quantum wells [Fig. 1(b)]. A decrease in the current is expected throughout this regime since the spatial overlap between the Stark-ladder states decreases with increasing field and with it the matrix element for transitions.⁹ Complete localization leading to Stark-ladder quantization was shown by the optical experiments of Mendez

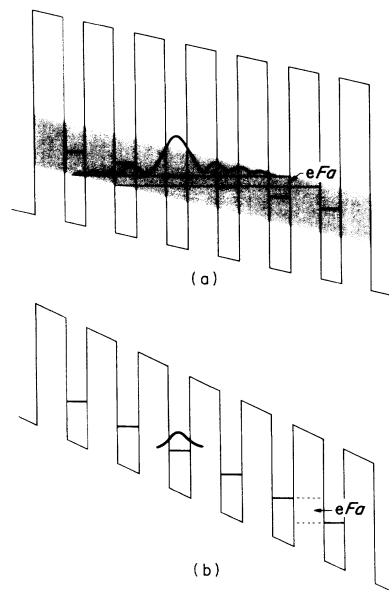


FIG. 1. Schematic conduction-band diagram of a heterojunction superlattice with an applied field: (a) electronic states extend over several periods and can be broadened by scattering into a band (shaded region) if Eq. (1) is not satisfied; (b) at very high biases [defined by Eq. (2)], electronic states are confined to single wells.

and co-workers^{10,11} and Voisin *et al.*¹² These experiments also clearly demonstrate the progressive nature of electric-field-induced localization. The question then arises, what is the threshold for localization?

Localization will occur when the energy levels of the Stark ladder can be resolved. In the presence of collisions this happens when their separation is greater than the collision broadening, i.e., $eaF > \hbar/\tau$. Therefore, in this physical picture, the threshold for the observation of NDC is $F > \hbar/ea\tau$. This is the same field calculated by Esaki and Tsu for the onset of NDC in a SL [Eq. (1)]. In fact, these two pictures for NDC are equivalent since the Stark-ladder states [Fig. 1(a)] arise from the interference between the forward-propagating and the Bragg-reflected wave. [Concerning the k -space derivation of Eq. (1) by Esaki and Tsu,¹ it should be noted that their approach is valid for fields F such that $eaF \ll \Delta E$, so that a semiclassical treatment is applicable.] Yakovlev¹³ investigated the conductivity of electrons in semiconductors with narrow (~ 0.1 eV) bands in strong electric fields. Although this paper was written before the introduction of the SL concept, its results are applicable to describe transport in these structures. Yakovlev indeed found that for fields satisfying Eq. (1), the conductivity decreases with increasing field. Moreover, as expected from the above discussion, his results are identical to the asymptotic results found by Tsu and Döhler.⁴

These theoretical predictions are experimentally verifiable by simply measuring the current-voltage characteristics of SL's: Starting at a bias defined by Eq. (1), a wide region where the current decreases with increasing voltage would be the signature of the localization. This observation, however, has not been reported yet.¹⁴ Recently, negative differential velocity (*not* negative differential conductance) has been inferred from microwave measurements in GaAs/AlAs SL's (Ref. 7) and attributed to the Esaki-Tsu mechanism.

In our opinion, one of the main problems hindering the experimental study of electronic transport in SL's has been the interdependence of the intensity of the current injected and the field present in the SL which is unavoidable in the two-terminal structures studied so far. At higher fields the large current densities injected make the field in the SL nonuniform and cause the formation of high-field domains.^{15,16} Therefore we designed a three-terminal structure that could simulate as closely as possible the "ideal" situation: a monoenergetic beam of electrons of constant-flux current impinging on the SL, independent of the value of the field in the SL. The equilibrium band diagram of our structure is schematically drawn in Fig. 2(a). The forward-biased p - n "emitter" heterojunction provides a controllable source of current independent of the reverse bias applied to the "collector" heterojunction which in turn controls the field in the SL. By measuring the collector current at constant-emitter current we can test the "intrinsic" SL transport proper-

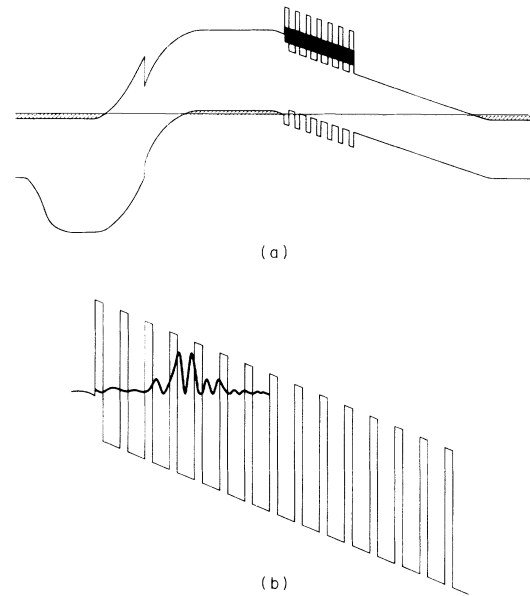


FIG. 2. (a) Energy-band diagram (not to scale) of the samples studied. (b) Conduction-band diagram of sample *A* at a bias such that a quasistate supported by a subset of the superlattice of thickness equal to the electron coherence length enhances electronic transport. The solid curve represents the calculated wave function corresponding to the peak at 10.9 V.

ties as a function of a uniform SL field avoiding the complications mentioned above. The undoped collector region between the SL and the contacted n^+ layer serves the purpose of scaling the applied bias.

The structures were grown by molecular-beam epitaxy lattice matched on an undoped InP substrate. The growth started with a 4955-Å $\text{Ga}_{0.47}\text{In}_{0.53}\text{As}$ buffer layer doped $n^+ = 1 \times 10^{18} \text{ cm}^{-3}$ followed by a 5945-Å-thick $\text{Ga}_{0.47}\text{In}_{0.53}\text{As}$ undoped collector region. The SL was then grown followed by a 5000-Å $\text{Al}_{0.163}\text{Ga}_{0.312}\text{In}_{0.525}\text{As}$ layer doped $p^+ = 5 \times 10^{18} \text{ cm}^{-3}$. Finally, 850-Å $\text{Al}_{0.48}\text{In}_{0.52}\text{As}$ $n^+ = 5 \times 10^{17} \text{ cm}^{-3}$ was grown separated by a 300-Å quaternary graded region from the $\text{Ga}_{0.47}\text{In}_{0.53}\text{As}$ $n^+ = 1 \times 10^{19} \text{ cm}^{-3}$ 2000-Å-thick cap contact layer. Two different undoped SL were studied. Structure *A* consists of 14 periods of 17-Å $\text{Al}_{0.48}\text{In}_{0.52}\text{As}/37$ -Å $\text{Ga}_{0.47}\text{In}_{0.53}\text{As}$. Structure *B* of 9 periods 23-Å $\text{Al}_{0.48}\text{In}_{0.52}\text{As}/36$ -Å $\text{Ga}_{0.47}\text{In}_{0.53}\text{As}$. The layer thicknesses were verified by transmission electron microscopy. Circular mesas were wet etched (diameter of the SL region $\approx 127 \mu\text{m}$) and Ohmic contacts were provided to the doped regions. The low-background doping of the collector layer guarantees a uniform field across the SL length ($< 1000 \text{ \AA}$) in the region of reverse bias of our experiments.

We modeled the SL's in the envelope-function approximation taking into account energy-band nonparabolicity.¹⁷ In structure *A* the calculated ground-state miniband dispersion is $\Delta E_A \approx 115 \text{ meV}$ and its bottom lies at

$E_0^A \approx 130$ meV, while in structure *B*, $\Delta E_B \approx 80$ meV and $E_0^B \approx 154$ meV. Therefore, in order to inject electrons into the miniband, the composition of the *p*-doped quaternary layer was chosen to be $\text{Al}_{0.163}\text{Ga}_{0.312}\text{In}_{0.525}\text{As}$. Assuming a linear *x* dependence for the $\text{Al}_x\text{Ga}_{0.475-x}\text{In}_{0.525}\text{As}/\text{Ga}_{0.47}\text{In}_{0.53}\text{As}$ conduction-band discontinuity, this corresponds to a conduction-band offset of ≈ 180 meV, roughly the center of the minibands (see Fig. 2). This favors the observation of NDC by Bragg diffraction since electrons are already near the negative-mass region of the miniband. The thickness of this layer is such that all the emitter electrons thermalize before impinging on the SL. Note that for both samples, the ground-state miniband is wide enough to ensure the absence of localization due to fluctuations.¹⁸ Moreover, the large energy separation ($\Delta E_s \approx 200$ meV in both samples) between the ground and first excited minibands ensures that Zener tunneling will not be possible in our structures for $F < \Delta E_s/eL \approx 30$ kV/cm (for both samples), where *L* is the total length of the SL.

The collector current density as a function of the collector-junction bias at constant-emitter current is shown in Fig. 3 for both samples. (The amplified scale has been chosen to clearly show the structure presented by the curves. The initial steeply rising region shows no features.) No space-charge effects are present in our structure. In fact, by taking into account the electron velocity in the miniband regime,⁶ one obtains an upper

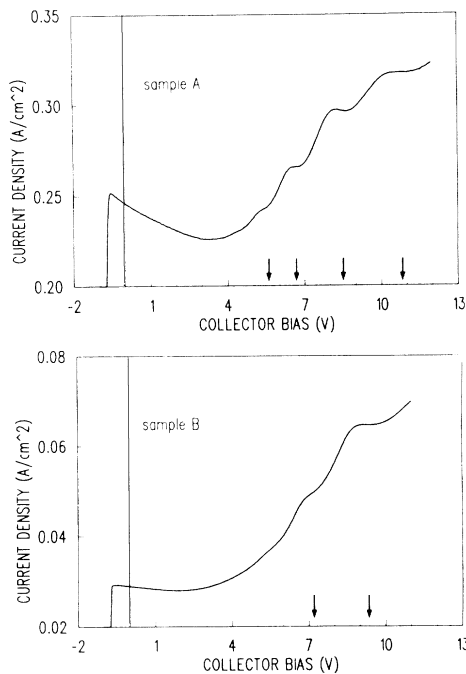


FIG. 3. Collector current density as a function of the collector bias at constant-emitter current ($I_E = 0.39$ A/cm²) for samples *A* (top) and *B* (bottom). Both measurements were performed at $T = 15$ K. The features presented by the characteristics were visible up to temperatures as high as 200 K. The arrows indicate the calculated bias positions of the resonances.

limit for the carrier density of 10^{12} cm⁻³. Moreover, this is proved by the experimental fact that by varying the emitter current, and therefore the electron flux incident on the SL, the collector current is simply scaled while the voltage positions of the relevant features are not altered. The current monotonically decreases in a wide-bias range. As discussed above, this is the experimental manifestation of localization. It constitutes its first direct observation in a transport measurement. The threshold for the onset of NDC can be determined by subtracting the forward-biased collector-junction dark current to the measured characteristics; it is $F \approx 3$ kV/cm, for both samples.¹⁹ This value is consistent with Eq. (1) taking $\tau \approx 4 \times 10^{-13}$ s, an adequate value for intrasubband scattering time²⁰ at these low fields.²⁰ This threshold value is much lower (a factor of 10) than the minimum field required for interminiband tunneling, as required for the observability of NDC.¹ It is also important to note that in our bipolar-transistor structure one cannot observe NDC by intervalley transfer in conditions of constant current injection. In these conditions, in fact, the decrease in velocity caused by the higher effective mass of the satellite valleys is compensated by an increase in the carrier density; the collector current is therefore not altered. On the other hand, the present NDC mechanism can be observed since the Bragg-reflected electrons in the negative-mass region of the minizone give rise to an opposite flux so that the collector current decreases while the base current increases to maintain a constant emitter bias. No NDC is observed in similar AlInAs/GaInAs structures without a SL in the collector.

The slope continues to be negative for fields corresponding to wave-function confinement over few ($\sim 3-4$ for both samples) wells where the characteristics exhibit a minimum.

The presence of the minimum indicates that, at sufficiently high bias, other paths can enhance electronic transport and become dominant in our structure. First, an exponentially increasing Fowler-Nordheim current through the SL seen as an effective medium is to be expected.²¹ More importantly, on this monotonically increasing background, several peaks are observed. To understand their physical origin, let us recall that in this field range, new states can arise from the mixing between Stark-ladder states originally belonging to different minibands or between the latter and resonances in the classical continuum above the SL barriers. In the case of transport in a SL without collision, these transmission resonances are determined by the whole SL. In the presence of collisions, however, they are determined by subsets of the SL of thickness equal to the electron coherence length. This is illustrated in Fig. 2(b) where one such state is shown for sample *A*. The electron coherence length must therefore be explicitly considered and can be included through the electron mean free path λ . In fact, the fraction of electrons that will tunnel

coherently for exactly n periods of the SL is equal to $e^{-na/\lambda}(1 - e^{-a/\lambda})$, and the corresponding transmission will be indicated by $T_n(F)$. The overall transmission coefficient is therefore given by

$$T(F) = \sum_{n=1}^{n_T-1} e^{-na/\lambda}(1 - e^{-a/\lambda})T_n(F) + e^{-n_T a/\lambda}T_{n_T}(F), \quad (3)$$

where n_T is the total number of wells. A fraction $1 - T(F)$ of the impinging electrons are therefore reflected back into the p -doped layer and recombine. The remaining electrons are injected into the SL. Their "history" after the first scattering event is immaterial since in our steady-state situation all electrons injected into the SL reach the collector contact. Excellent agreement is found between calculated and experimental position of the peaks with $\lambda \approx 300 \text{ \AA}$. The calculated (experimental) biases for sample *A* are 5.6 (5.5), 6.7 (6.7), 8.5 (8.5), 10.9 V (10.9 V); for sample *B*, 7.1 (7.1), 9.3 V (9.3 V). λ is obviously F dependent, but we found that our results do not change appreciably with λ in the range 200–400 \AA . On the contrary, allowing for an infinite coherence length (i.e., electrons traversing ballistically the entire SL) leads to a much larger number of calculated resonances. As mentioned above, band nonparabolicities were included, the nonparabolicity parameter γ was taken equal to $1.7 \times 10^{-18} \text{ m}^2$.²²

It is important to note the connection between our results and the optical experiments of Mendez and co-workers.^{10,11} These authors observed transitions between conduction-band states of spatial extent equal to the coherence length and totally localized valence-band states.

In conclusion, we have studied and modeled the properties of perpendicular transport in heterojunction SL's. Esaki-Tsu mechanism and field-induced localization have been analyzed critically. Their physical equivalence has been discussed and verified experimentally. At high fields, the dominant role of scattering-selected resonances has been presented and modeled.

The authors gratefully acknowledge stimulating discussions with A. S. Vengurlekar.

¹L. Esaki and R. Tsu, IBM J. Res. Develop. **14**, 61 (1970). Later, with a different theoretical approach, the same phenomenon was studied by M. Büttiker and H. Thomas, Phys. Rev. Lett. **38**, 78 (1977).

²F. Capasso and S. Datta, Phys. Today **43**, No. 2, 74 (1990).

For NDC effects observed in surface SL's, see D. K. Ferry, in *Physics of Quantum-Electron Devices*, edited by F. Capasso (Springer-Verlag, New York, 1990), Chap. 4.

³P. A. Lebowitz and R. Tsu, J. Appl. Phys. **41**, 2664 (1970).

⁴R. Tsu and G. Döhler, Phys. Rev. B **12**, 680 (1975).

⁵G. Döhler, R. Tsu, and L. Esaki, Solid State Commun. **17**, 317 (1975).

⁶F. Capasso, K. Mohammed, and A. Y. Cho, IEEE J. Quantum Electron. **22**, 1853 (1986).

⁷A. Sibille, J. F. Palmier, H. Wang, and F. Mollot, Phys. Rev. Lett. **64**, 52 (1990).

⁸G. Wannier, Phys. Rev. **117**, 432 (1960).

⁹R. F. Kazarinov and R. A. Suris, Fiz. Tekh. Poluprov. **5**, 797 (1971); **6**, 148 (1972) [Sov. Phys. Semicond. **5**, 707 (1971); **6**, 120 (1972)].

¹⁰E. E. Mendez, F. Agullo-Rueda, and J. M. Hong, Phys. Rev. Lett. **60**, 2426 (1988).

¹¹F. Agullo-Rueda, E. E. Mendez, and J. M. Hong, Phys. Rev. B **40**, 1357 (1989).

¹²P. Voisin, J. Bleuse, C. Bouche, S. Gaillard, C. Alibert, and A. Regreny, Phys. Rev. Lett. **61**, 1639 (1988).

¹³V. A. Yakovlev, Fiz. Tverd. Tela **3**, 1983 (1962) [Sov. Phys. Solid State **3**, 1442 (1962)].

¹⁴Previously negative differential photoconductance in two-terminal SL structures was tentatively attributed to field-induced localization in the sense of Tsu and Döhler (Ref. 4). R. Tsu, L. L. Chang, A. Sai-Halasz, and L. Esaki, Phys. Rev. Lett. **34**, 1509 (1975); F. Capasso, K. Mohammed, and A. Y. Cho, Physica (Amsterdam) **134B&C**, 487 (1985); H. Schneider, K. van Klitzing, and K. Ploog, Europhys. Lett. **8**, 575 (1989).

¹⁵L. Esaki and L. L. Chang, Phys. Rev. Lett. **33**, 495 (1974).

¹⁶K. K. Choi, B. F. Levine, R. J. Malik, J. Walker, and C. G. Bethea, Phys. Rev. B **35**, 4172 (1987).

¹⁷D. F. Nelson, R. C. Miller, and D. A. Kleinman, Phys. Rev. B **35**, 7770 (1987).

¹⁸F. Capasso, K. Mohammed, A. Y. Cho, R. Hull, and A. L. Hutchinson, Phys. Rev. Lett. **55**, 1152 (1985).

¹⁹The field in the SL is $F = (V + V_{bi})/L$, where L is the width of the intrinsic collector region and the built-in potential $V_{bi} \approx 0.92 \text{ V}$.

²⁰D. C. Herbert, Semicond. Sci. Technol. **3**, 101 (1988).

²¹The reverse-bias leakage current of the collector junction is negligible in the bias and temperature range of our experiments.

²²Experimental measurements on γ give results in a rather broad range, $\gamma = 1.3 \times 10^{-18} \text{ m}^2$ was reported by L. Eaves, F. W. Sheard, and G. A. Toombs, in *Physics of Quantum-Electron Devices*, edited by F. Capasso (Springer-Verlag, New York, 1990); a value 4 times higher was found by C. K. Sarkar, R. J. Nicholas, J. C. Portal, M. Razeghi, J. Chevrier, and J. Massies, J. Phys. C **18**, 2667 (1985). The value indicated was chosen to optimize the fit.

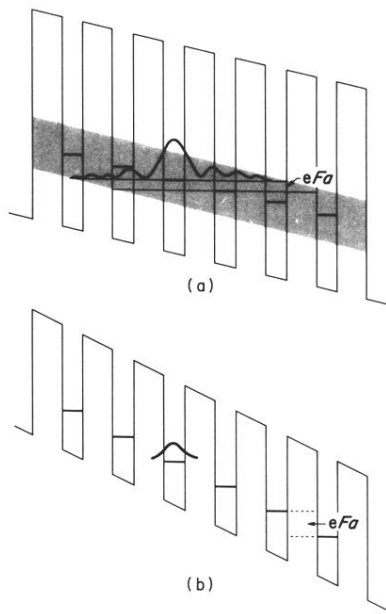


FIG. 1. Schematic conduction-band diagram of a heterojunction superlattice with an applied field: (a) electronic states extend over several periods and can be broadened by scattering into a band (shaded region) if Eq. (1) is not satisfied; (b) at very high biases [defined by Eq. (2)], electronic states are confined to single wells.

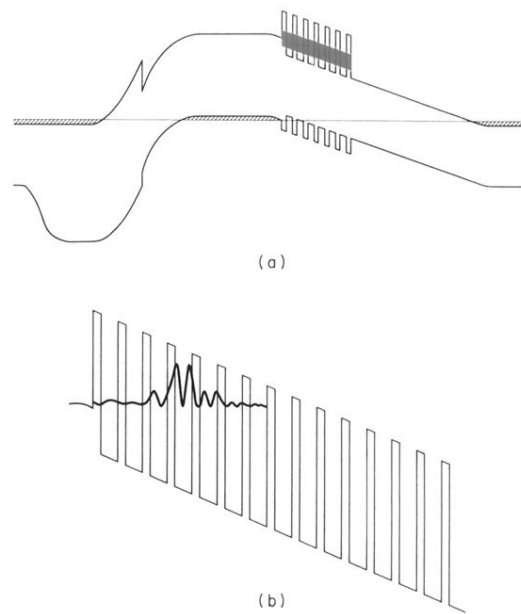


FIG. 2. (a) Energy-band diagram (not to scale) of the samples studied. (b) Conduction-band diagram of sample *A* at a bias such that a quasistate supported by a subset of the superlattice of thickness equal to the electron coherence length enhances electronic transport. The solid curve represents the calculated wave function corresponding to the peak at 10.9 V.